

Experimental analysis of cyclic loading on a cohesionless granular system

Zhongwei Bi¹ · Wanfu Huang¹ · Qicheng Sun² · Shuwei Sun³

Received: 29 October 2013 / Published online: 26 February 2016
© Springer-Verlag Berlin Heidelberg 2016

Abstract The cyclic loading mechanical response of dense granular materials under biaxial compressions was experimentally investigated. Ratcheting occurred and evolved throughout the experiment. The results suggest that permanent displacement primarily occurs during the first cycle; the generation of ratcheting is principally driven by the occurrence of stick–slip events and the changes in porosity. In different cycles, the occurrence of stick–slip events obeys the power law relationship, and the change in porosity tends to approach a homogenous state. Simultaneously, the magnitude of the initial force plays an important role for increasing ratcheting in granular system.

Keywords Granular materials · Ratcheting · Stick–slip · Cyclic loading

1 Introduction

Granular materials are collections of discrete macroscopic particles. They typically interact with each other only within short distances, mainly through collisions and contacts. Most common examples include food products, such as rice, corn, and breakfast cereal flakes, and building materials such as sand, gravel, and soil, and chemicals such as coal, plastics,

and pharmaceuticals. Colloids (e.g. grains in solvent and, pastes) can be classified as granular materials, but only dry cohesionless granular matters are considered in this paper. Despite their seeming simplicity, the behavior of granular materials differs from that of any of the other familiar forms of matter: solids, liquids, or gases. The behavior involves stick–slip motion, dilatancy, pattern formation, segregation, as well as ratcheting and anisotropy among many others [1, 2].

A particularly intriguing phenomenon in granular systems is the so-called ratcheting effect, this effect is known as granular ratcheting, and it refers to the constant accumulation of permanent displacement (or strain) per cycle, when the granular sample is subjected to load–unload force (stress) cycles. Herrmann [3], Peijun Guo et al. [4] have done a lot of research on the mechanical properties of granular system under cyclic loading; furthermore, Peijun Guo has done some research on the influence of confining pressure, deviatoric stress and micromechanical parameters. Some experimental data, suggests that the rebound modulus change is in line with the change of loading cyclic, but not sensitive to the change of confined forces; for example [5,6]. Moreover, some pavement designers thought that, if a 2D granular packing of discs were subjected to stress-controlled cyclic loading, the displacement accumulations were identified as shakedown, or ratcheting, depending on the amplitude of the stress variations. This particular phenomenon has been intensively investigated in 2D (Alonso-Marroquin et al. 2004; Garcia-Rojo et al. 2004); Further; Md. Mahmud Sazzad and Kiichi Suzuki [7] have investigated the anisotropy characteristics of non-spherical particles under cyclic loading. McNamara and Garcia-Rojo [8] have studied the origin of ratcheting through a combination of 16 particles. Besides, a large number of personnel have also carried out a similar study.

✉ Zhongwei Bi
bizhongwei1976@163.com

¹ Faculty of Resource and Environmental Engineering, Jiangxi University of Science and Technology, Ganzhou 341000, China

² State Key Laboratory of Hydroscience and Engineering, Tsinghua University, Beijing 100084, China

³ Faculty of Resources and safety Engineering, China University of Mining and Technology, Beijing, China

Although there is wide experimental evidence describing the accumulation of permanent deformation under cyclic loading, it is not clear whether this effect remains for small loading amplitudes, or if there is a certain regime where the material behaves perfectly elastic [9]. It is still also not clearly understood what the role of micromechanical processes, such as sliding, crushing and wearing of the grains, are in the accumulation of plastic deformation with the number of cycles [10].

Here we present experimental evidence of the ratcheting effect on assemblies of densely packed circular particles. This can be detected at the micromechanical level by a ratchet-like behavior at the contacts. This effect excludes the existence of the ideal elastic regime of cohesionless granular materials [11].

2 Experimental devices and results

2.1 Experimental devices

The experimental system consists of a tri-disperse mixture of 2500 large (diameter $D = 1.0 \pm 0.025$ cm), 2500 middle ($D = 0.8 \pm 0.025$ cm) and 2500 small ($d = 0.6 \pm 0.025$ cm) polymer disks with a thickness of 0.3 cm, that are birefringent under stress (photoelastic) (Fig. 1). They are made of polycarbonate elastomer, and their Young modulus is $E = 3.15 \times 10^5$ Pa, Poisson coefficient is $\lambda = 0.36$ and friction coefficient is $\mu = 0.2$. The disks are placed in an 80 cm \times 80 cm chamber. The upper (the axial) and left boundaries can be moved freely, the other boundaries were fixed. The axial load was applied using electro-motor loading system and measured at a load cell accuracy (0.2 N) inside the pressure cell below the lower specimen end plate. The axial displacement of the boundary was monitored using a displacement transducer with an accuracy of 0.001 mm

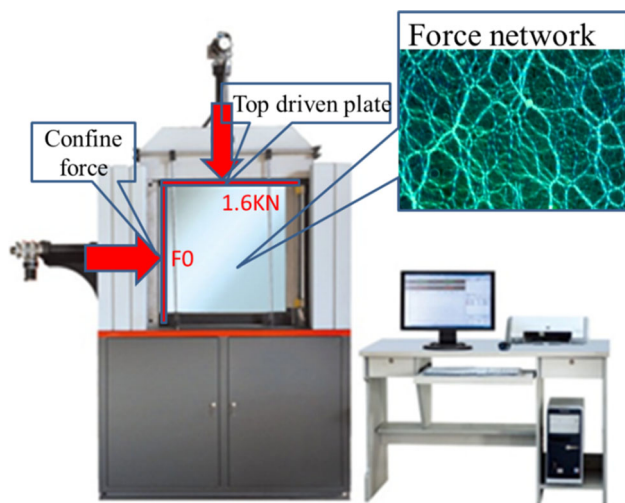


Fig. 1 Experimental schematic

that was fixed to the load piston. Visual measurements were taken using a Nikon D-90 camera (12.3 megapixel resolution) to determine the yield positions and displacements of the individual disks, as well as the stresses inferred from the photo-elastic response of the disks [12]. Each image captured roughly 5000 particles located around the center of the cell, roughly 60% of the total number of particles. The system is imaged through crossed circular polarizers. We determined that the local disk contacts have a stress above our experimental light intensity threshold (corresponding to about 1 N) and satisfy local force balance constraints, for the forces which are less than 1 N, the Tardy compensation method is used for compensation. The entire stress chain network satisfies physical constraints and provides a good characterization of the distribution of local forces to complement the pressure measurements. To prevent generating plasticity in the materials, the test was first done to a single particle. After the maximum force (1.6 kN) was applied, the maximum deformation of the particles did not exceed 1.8% of the minimum particle diameter; therefore, the deformation of the particles was complete elastic deformation during the loading process, which can be fully recovered after unloading, meaning, there was no plastic deformation.

2.2 Experimental programs

A three-part experimental design was created to analyze ratcheting (Table 1).

1st type: cyclic loading with a constant amplitude (S1, S2, S4, S5, S7, S8). Initially, the samples were isotropically compressed until the confined forces reach to $F_0(0.4, 0.6, 0.8)$. Then, the samples are subjected to axial loading–unloading cycles, the loading interval is defined as A, [0.4, 0.8] for S1 and S2, [0.6, 1.2] for S4 and S5, [0.8, 1.6] for S7 and S8, the cycle index defined as N, and the loading rate is 0.2 N/S for all.

2nd type: cyclic loading with varied amplitudes (S3, S6). Initially, the samples were isotropically compressed until the confined forces reached $F_0(0.4, 0.6, 0.8)$. Then, the samples were subjected to axial loading–unloading cycles; the loading interval is defined as A, [0.4, 0.8] for S3, [0.6, 1.2] for S6, and the cycle index defined as N. Finally, the cycling amplitude was increased to interval A1, [0.6, 1.2] and [0.8, 1.6] for S3, [0.8, 1.6] for S6; the cycle index was kept as N.

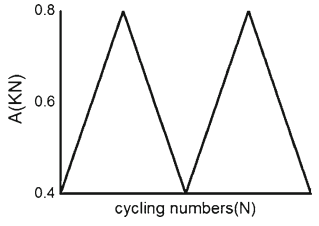
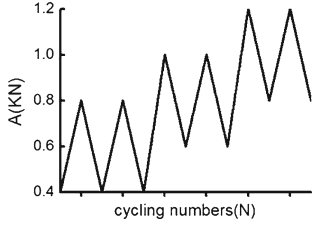
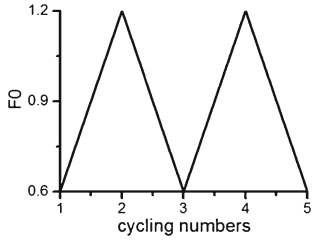
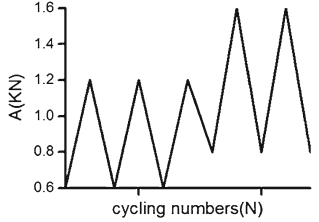
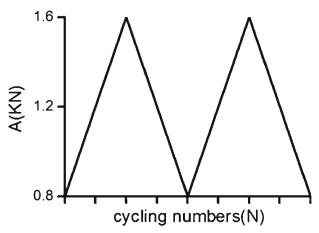
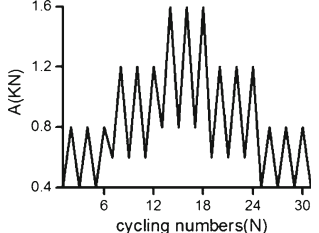
3rd type: cyclic loading under varied amplitude (S9). S9 was loaded three times under the conditions of 0.6 ± 0.2 , 0.9 ± 0.3 , 1.2 ± 0.4 , 0.9 ± 0.3 , and 0.6 ± 0.2 kN.

2.3 Experimental results

Figure 2 shows the examples of the force-displacement plots.

The results show that there is no elastic stage in granular system (Fig. 2). The hysteresis loops are not closed in

Table 1 Ratcheting experimental datasheet

Sample number	Confined force F_0 (kN)	Cyclic number (N) and cyclic amplitude (A)	Load schematic
S1 S2	0.4	N=40 (A=0.4) N=40 (A=0.4)	
S3	0.4 0.6 0.8	N=30 (A=0.4) N=3 (A=0.6) N=3 (A=0.8)	
S4 S5	0.6	N=20 (A=0.6) N=30 (A=0.6)	
S6	0.6 0.8	N=20 (A=0.6) N=10 (A=0.8)	
S7 S8	0.8	N=20 (A=0.8) N=20 (A=0.8)	
S9	0.4 0.6 0.8 0.6 0.4	N=3 (A=0.4) N=3 (A=0.6) N=3 (A=0.8) N=3 (A=0.6) N=3 (A=0.4)	

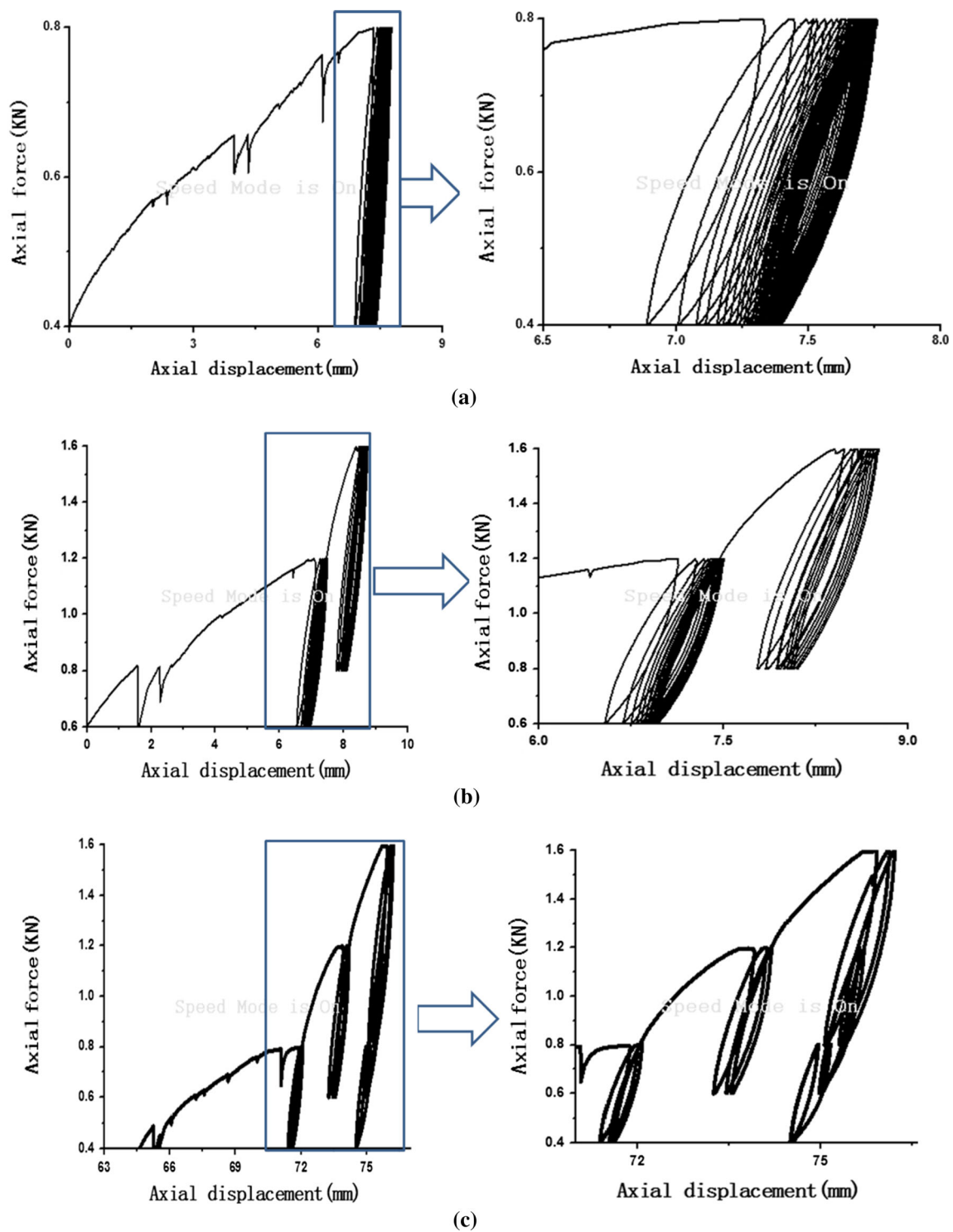


Fig. 2 Force-displacement curves of the system, **a** Force-displacement curve of S1. **b** Force-displacement curve of S6. **c** Force-displacement curve of S9

the initial stage or later stage, and, there is a significant ratcheting effect. Meanwhile, the hysteresis loops are not identical, not closed from beginning to end; the opening of the first hysteresis loop is relatively large, but the subsequent loops are relatively small. Further, the shape of the hystere-

sis loop changes from an oval to a leaf tip as the number of cycles increase. Additionally, the structure (arrangement mode) of the particles controls the permanent displacement of the first cycle in granular system. Since the samples are randomly selected and put into the chamber, there are no

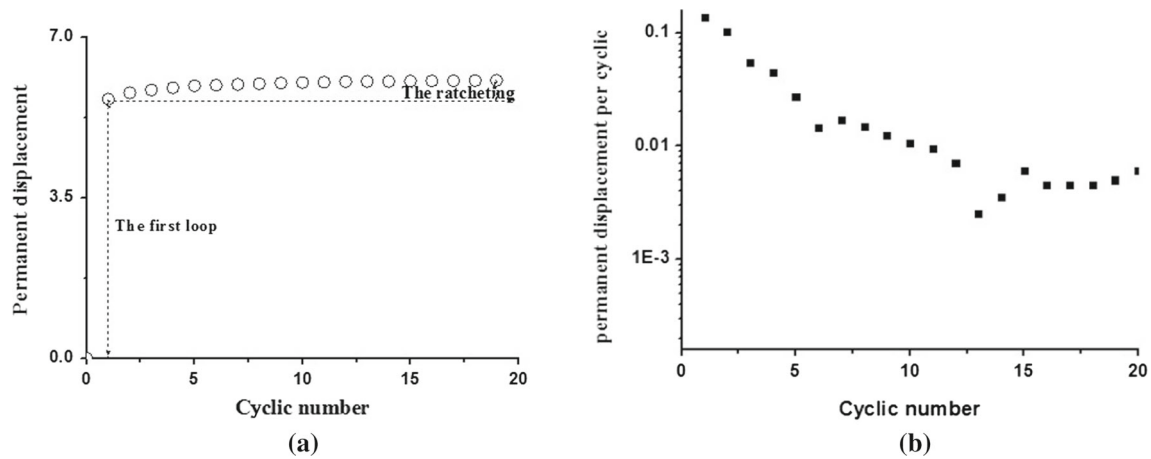


Fig. 3 Ratcheting phenomenon of S1, **a** permanent displacement (incl. 1st cycle). **b** Permanent displacement per cycle (excl. 1st cycle)

identical samples (For the preparation of samples, first pull out the chamber, make the customized strip-typed hopper opening match with the opening of the top driven plate, then spatter the particles in plate form from top to down. When the altitude can meet the experimental requirement, push in the chamber). Therefore, the unclosed degree of the first hysteresis loop has a big difference and with no obvious law. However, the permanent displacement generated in the first cycle accounts for approximately 90% of the entire cycling process, indicating that the permanent displacement and energy consumption in the first cycle are very large. After entering the second cycle, the accumulated displacement per cycle becomes smaller until an approximately constant value ($10e-3$ mm) is reached (Fig. 3a). The displacement response consists of short time regimes (<7 cycles) with a rapid accumulation of displacement (permanent displacement per cycle $>10e-2$), and longtime ratcheting regimes (until ratcheting disappeared) with a constant accumulation displacement rate of around $10e-3$ mm per cycle.

The permanent displacement accumulation per cycle becomes independent from the number of cycles following a short transient regime (Fig. 3b). From a micromechanical point of view, the observed macroscopic strains are associated to the evolution of the contact network, which in turn is due to the relative sliding and rotation of particles at contacts. However, the focus of this study is on particle sliding.

3 The origin of ratcheting

3.1 Stick–slip phenomenon

The interaction between particles is mainly through contacts, and these contacts obey Moore–Coulomb’s law [13–15]. Coulomb’s law of friction is a non-smooth law in that the friction force and sliding velocity at a contact are not related

as a function. Many experiments have explored the dynamic characteristics of slowly driven granular systems, such as the strong force fluctuation due to the formation of stress chains and friction that results in stick–slip motions. However, these studies did not focus on the statistical aspects of the sheared granular media, and there are few records that describe cyclic loading. However, power law distribution of responses has been observed in sheared tapioca grains in annular cells [16, 17].

McNamara and Garcia-Rojo have carried out a detailed study on cyclic loading, and thought that stick–slip is the cause of ratcheting. However, these studies only analyzed the ratcheting phenomenon after the second cycle, and no studies have examined this effect during the first cycle. In order to analyze the stick–slip phenomenon, the first and second S7 cycles in the force rising phase were analyzed because it has a large force variation range [0.8, 1.6]. The relationship between the axial displacement and the force increases slowly, then drops suddenly, indicating that there is a stick–slip event occurring during the loading process (Fig. 2a). By dividing the displacement difference at every jump by the time difference we get the (discrete) velocity of the top-driven plate, shown in Fig. 4a, b. The changes in velocity of the top driven plate demonstrate a series of events along with the time (Fig. 4a, b). The velocity of the top driven plate fluctuates more during the first cycle than in the second cycle; the fluctuation interval is [0, 0.3] in the first cycle, while [0, 0.04] in the second cycle, only 1/10 of that in the first cycle. This indicates that, along with the ongoing cycles, the velocity of top driven plate is approaching a stable state. It further suggests that the granular microstructure has settled into a final configuration. Under the same time span, there were six fluctuations in the second loading cycle, and 36 in the first loading (Fig. 4c, d). This indicates that under some confined forces, with the increase of loading times, the granular system becomes more stable, and ratcheting regime

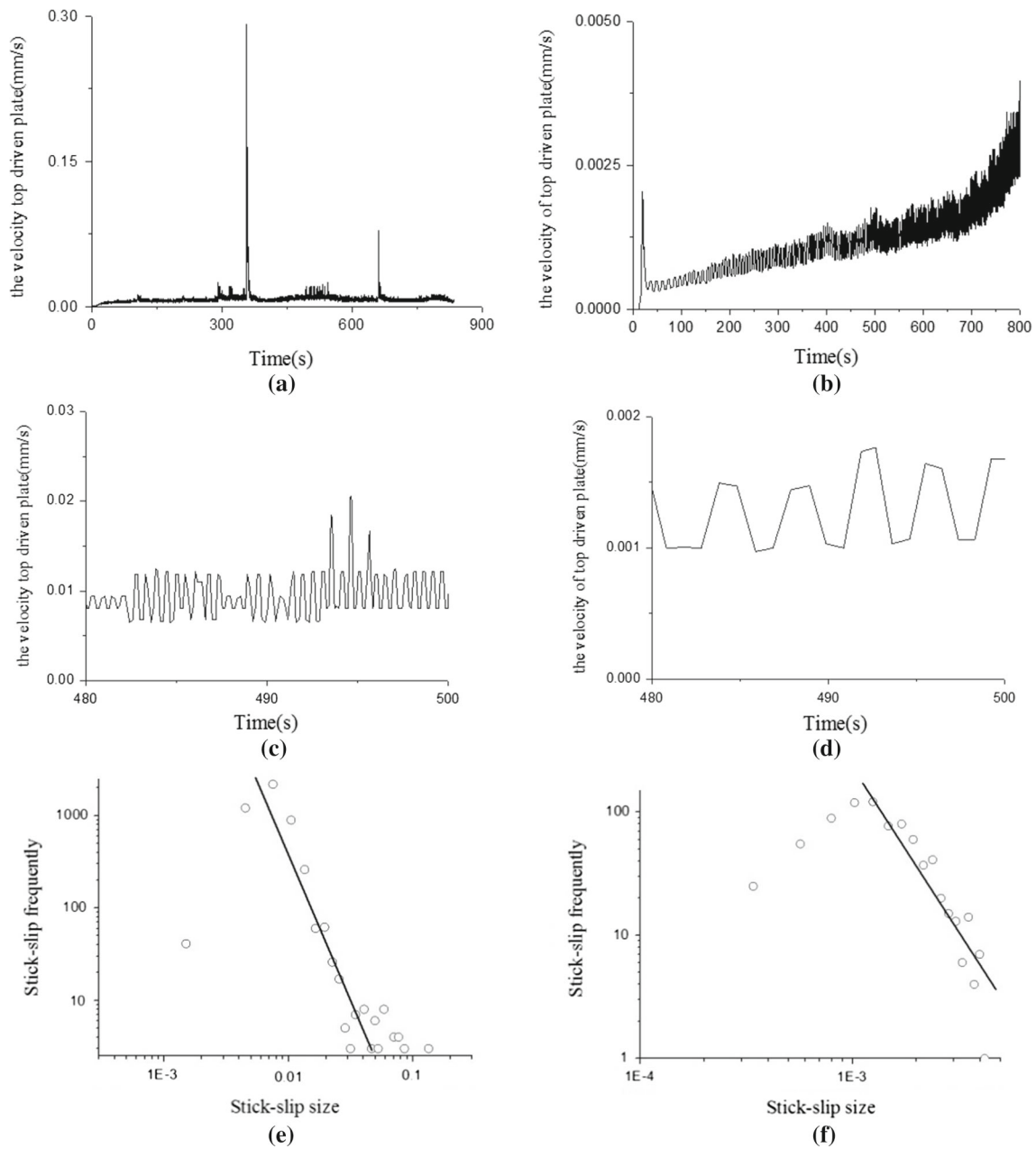


Fig. 4 Time versus velocity of top driven plate and stick–slip size versus frequency in 1st and 2nd cycle, **a** time versus velocity of top driven plate in 1st cycle. **b** Time versus velocity of top driven plate in 2nd cycle.

c Zoom-in of **a**. **d** Zoom-in of **b**. **e** Stick–slip size versus frequency in 1st cycle. **f** Stick–slip size versus frequency in 2nd cycle

becomes smaller. However, before the sliding events occur, the motions develop in a periodic fashion (Fig. 4c, d).

In order to analyze the distribution of the stick–slip motions, each stick–slip associated fluctuation was denoted as s . Make statistics to s , the statistical interval is $[0, 0.3]$ in the first cycle and $[0, 0.04]$ in the second cycle. These distributions are showed in Fig. 4e, f. The s distribution tendency of all samples is similar, and each curve follows a quasi-power law behavior.

The distribution of the stick–slip events in the first cycle is more broad than it is in the second cycle, indicating that

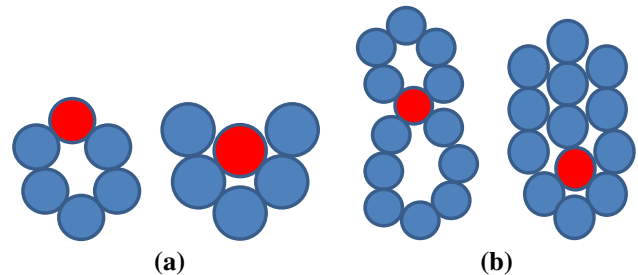


Fig. 5 Stick–slip schematic, **a** small stick–slip. **b** Large stick–slip

the porosity non-uniformity of the granular system affects stick–slip occurrences (Fig. 4). Following the first cycle, the fluctuation time of the stick–slip reduces, and the permanent displacement diminishes, indicating that the porosity non-uniformity of granular system becomes increasingly weak.

The stick–slips were classified as type I and type II according to the size of the torque [18]. Type II corresponds to the stick–slip phenomenon in the first cycle because it exhibits asymmetric fluctuations that are “saw-tooth” in nature. Type I corresponds to the velocity in the second cycle because it has predominantly symmetrical fluctuations of stick-increasing and slip-decreasing events. It was also found that, with regard to small slips, sometimes the sound and motion of the particles due to adjustment can be seen and heard. However, they are not always observed. Partial particles had small adjustment during this time, and only some particles changed their positioning (Fig. 4a). The motion of the particles exhibits a significant overall stick–slip in large slips, and louder sound can be heard. Combined with numerical image processing, it can be seen that the granular system experienced significant macroeconomic adjustments at this time.

Different levels of stick–slip phenomenon can be explained using the schematics (Fig. 5). The red particles are the key particles; when the red particle slips, it cannot lead to the movement or adjustment of the surrounding particles. This event is called a small stick–slip (Fig. 5a). When the red particle slips and it affects the movement of the surrounding particles, and leads to the adjustment of two or more particle clusters, and even causes the movement or adjustment throughout the granular system, this is called as large stick–slip (Fig. 5b). The large stick–slip is associated with dramatic fluctuations in the force curve.

McNamara studied the permanent displacement caused by stick–slips of particles, indicating that if there are no sliding contacts, then the trajectories of particles are straight lines. Further, if there is no change in the displacement of the particles and they return to their original positions, no, and ratcheting does not occur. However, when the particles cannot return to their original positions, ratcheting occurs, and is in line with the findings from the experiment in this paper.

3.2 Porosity changes

Two studies have investigated force chain networks and the average coordination numbers [19,20]. These studies found that the normal and tangential forces obey a certain distribution following force fluctuation. However, few studies have examined these forces under porosity fluctuations. In numerical simulation processes, most studies generated some porosity samples using technology, and considered the pores of the granular system to uniform everywhere after a certain coarse-grained interval. However, it was found that, when

the divided interval includes 40 particles, there is still a large fluctuation in the porosity. Therefore, real granular systems have heterogeneous pores, making it is necessary to conduct research on the porosity fluctuation that results in permanent displacement. For example, in S4, obtaining digital images of the experimental samples under isotropic compression using a digital camera. Then, the images were equally divided into 2000×2000 pixel intervals, each interval including 40 particles more or less (Fig. 6a), through the image recognition and processing, and a porosity of 0.1823 was obtained. This technique can be used for any interval, and each interval has large porosity fluctuations. The average porosity of all experimental samples is 0.18. The interval vs. the porosity fluctuation shown in Fig. 6c, the fluctuation interval is $[-0.04, 0.045]$. At the beginning of isotropic compression, the porosity in each interval is unevenly distributed.

The permanent displacement of the granular system is 6.6 mm after the first S4 cycle. The porosity of the interval was reduced to 0.1820, indicating that the interval is under a compressed state (Fig. 6b). The average porosity of the granular system was reduced by 0.0003 after the first cycle, but the spatial distribution of the porosity was still uneven, with some fluctuations and an interval of $[-0.0204, 0.0213]$ (Fig. 6d). Overall, the homogeneity of the pores becomes smaller following cyclic processes, further indicating that the permanent displacement of the granular system is drive by the heterogeneous pores.

In order to illustrate the causes of permanent displacement, the change of porosity fluctuations in different intervals before and after each cycle was obtained (Fig. 6e). It was found that the change in porosity was not uniform, because some intervals were under a dense state, while others were under a sparse state. The black in Fig. 6e shows that the compaction degree of the pores under a dense state is greater than the average compaction degree. The red shows the compaction degree of porosity that is less than the average compaction degree, and white represents the compaction degree of porosity that equals the average compaction degree. Together, this indicates the structure of granular system changed during the different intervals. Combined with the stick–slip phenomenon in Fig. 5, it can be concluded the ratcheting effect is caused by structural adjustment of the granular system. The fluctuation of porosity in the different intervals follows a normal distribution, and the change in porosity for more than 70% of the intervals is the same as that of the overall samples (Fig. 6f). Only a few of the changes in porosity result in fluctuations that deviate from the overall samples, indicating that stick–slip phenomenon exists in partial intervals, and that these fluctuations result in significant ratcheting events in granular systems. After the tenth cycle, the porosity fluctuations of the granular system are within $[-0.0056, 0.0088]$, and the fluctuation region is reduced significantly, indicating that the porosity of the gran-

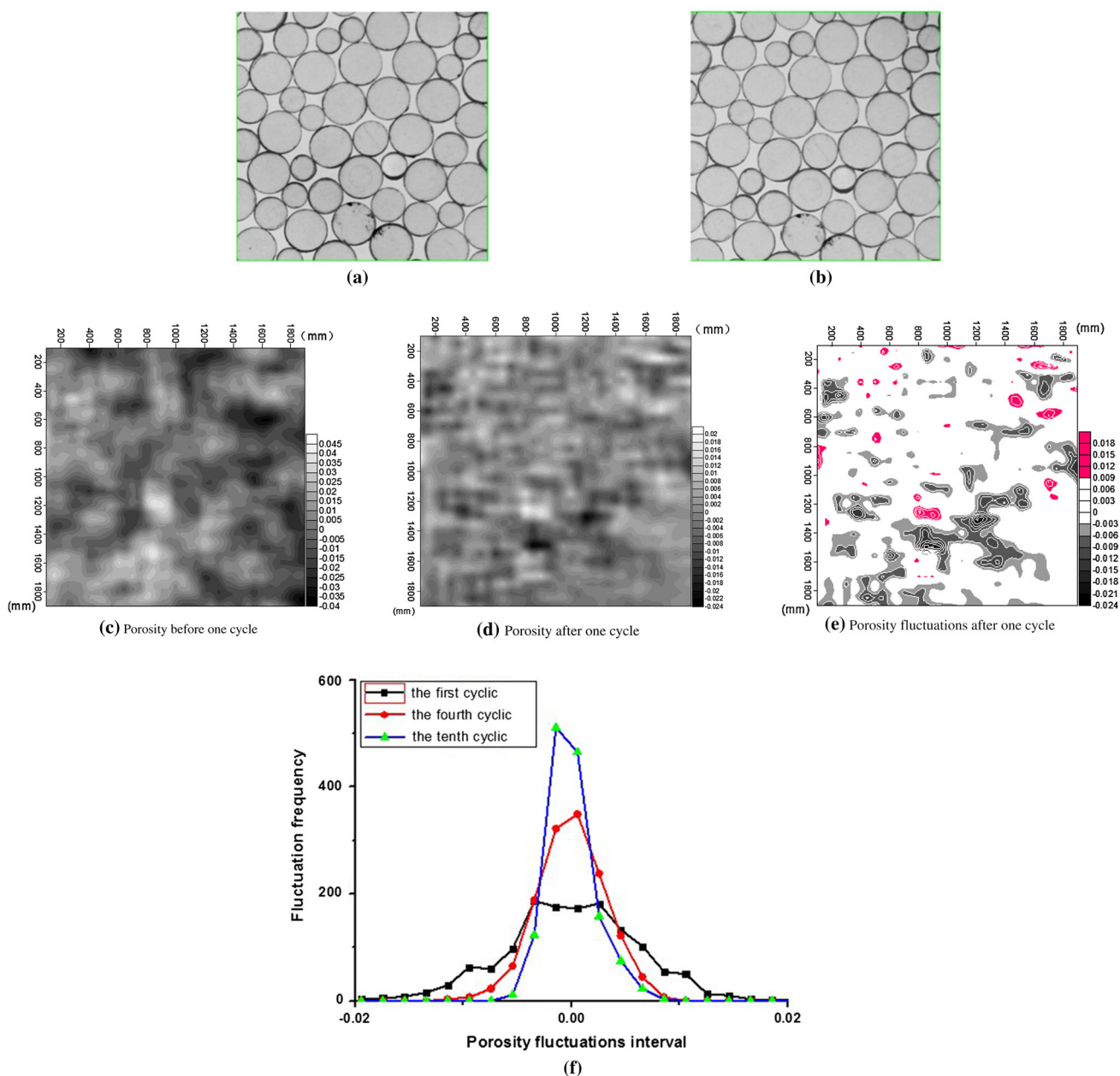


Fig. 6 The porosity variation, **a** snapshot before one cycle. **b** Snapshot after one cycle. **c** Porosity before one cycle. **d** Porosity after one cycle. **e** Porosity fluctuations after one cycle. **f** Varieties and distribution of porosity

ular system becomes more uniform, and the deformation of the granular system approaches affine deformation. This is shown by an increasing number of steep peaks on the curve, and increasingly smaller range distribution (Fig. 6f).

3.3 Displacement field

During the ratcheting regime, the accumulation of permanent displacement in each cycle at the stick–slip will be reflected in a displacement per cycle at the individual grains. It is of great interest to study the patterns that are created by the displacement field of all the grains.

During cyclic loading, the trajectory of a single particle is given by a constant, small displacement per cycle in the ratcheting regime, and a large displacement during the transition between two ratcheting regimes. Typically, the maximal displacement per cycle at the transition between the two ratcheting regimes is one or two orders of magnitude larger than that in a single ratcheting regime.

Figure 7 shows a snapshot of the particle displacement per cycle for these two cases. The most important remark of this flow is the formation of the vortex structures. An animation of this flow depicts a constant vorticity field during the ratch-

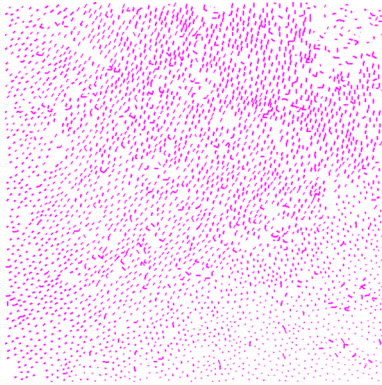


Fig. 7 The displacement gradient of granular matter

eting regime, and large vorticities during the transition of the two ratcheting regime. It was also observed that the vortex structures were created and destroyed during this transition.

Vorticity is linked with the nonvanishing asymmetric portion of the displacement gradient [21], and the strain tensor is not sufficient to provide a complete description of this convective motion during cyclic loading. An appropriate continuum description would require the introduction of additional degrees of freedom that take into account the vorticity. As in the case of the shear band formation, the Cosserat theory may be a good alternative [22].

4 Results

A grain scale investigation of the cyclic loading response of the packing of disks has been presented. In the quasistatic regime, we have shown the existence of long time regimes with an accumulation of permanent displacement per cycle, due to ratcheting motion at the stick–slip.

As the loading amplitude decreases, a smooth transition from the ratcheting to the shakedown regimes was observed, preventing the identification of a purely elastic regime. The granular ratcheting resulted from anisotropy induced by the loading on sliding contacts for small loading amplitudes.

The overall response of the polygonal packing under cyclic loading consists of a sequence of ratcheting regimes with a long duration, and a slow accumulation of deformation in the plastic. These regimes are separated by short regimes with large plastic deformations.

The analysis of the displacement field per cycle of the particles shows that each particle moves with constant displacement per cycle during the ratcheting regimes. These displacements form vortex-like structures, which remain during for the duration of the ratcheting regime.

Acknowledgments This work was supported by Chinese Postdoctoral Science Foundation (2014M550358)

References

- Alonso-Marroquín, F., Mühlhaus, H.B., Herrmann, H.J.: Micromechanical investigation of granular ratcheting using a discrete model of polygonal particles. *Particuology* **6**, 390–403 (2008)
- Bi, Z.W., Sun, Q.C., Jin, F., Zhang, M.: Numerical study on energy transformation in granular matter under biaxial compression. *Granul. Matter* **13**, 503–510 (2011)
- Alonso-Marroquín, F., Herrmann, H.J.: Ratcheting of granular materials. *Phys. Rev. Lett.* **92**, 054301 (2004)
- Guo, P., Emery, J.: Importance of strain level in evaluating resilient modulus of granular materials. *Int. J. Pavement Eng.* **12**(2), 187–199 (2011)
- Perez, I., Medina, L., Romana, M.G.: Permanent deformation models for a granular material used in road pavements. *Constr. Build. Mater.* **20**, 790–800 (2006)
- Tutumluer, E., Seyhan, U.: Laboratory determination of anisotropic aggregate resilient modulus using an innovative test device, pp. 13–21. *Transportation Research Record*, Transportation Research Board, Washington (1999)
- Sazzad, M.M., Suzuki, K.: Micromechanical behavior of granular materials with inherent anisotropy under cyclic loading using 2D DEM. *Granul. Matter* **12**, 597–605 (2010)
- McNamara, S., García-Rojo, R.: Microscopic origin of granular ratcheting. *Phys. Rev. E* **77**, 031304 (2008)
- Gudehus, G., Jiang, Y.M., Liu, M.: Seismo- and thermodynamics of granular solids. *Granul. Matter* **13**, 319–340 (2011)
- Lobo-Guerrero, S., Vallejo, L.E.: Discrete element method analysis of railtrack ballast degradation during cyclic loading. *Granul. Matter* **8**, 195–204 (2006)
- Calvetti, F., di Prisco, C.: Discrete numerical investigation of the ratcheting phenomenon in granular materials. *Comptes Rendus Math.* **338**(10), 604–614 (2010)
- Majmudar, T.S., Behringer, R.P.: Contact force measurements and stress induced anisotropy in granular materials. *Nature* **435**, 1079–1082 (2005)
- García-Rojo, R., Alonso-Marroquín, F., Herrmann, H.J.: Characterization of the material response in granular ratcheting. *Phys. Rev. E* **72**, 041302 (2005)
- Pena, A.A., Lizcano, A., Alonso-Marroquín, F., Herrmann, H.J.: Biaxial test simulations using a packing of polygonal particles. *Int. J. Numer. Anal. Methods Geomech.* **32**, 143–160 (2008)
- Luding, S.: Constitutive relations for the shear band evolution in granular matter under large strain. *Particuology* **6**, 501–505 (2008)
- Dalton, F., Corcoran, D.: Self-organized criticality in a sheared granular stick-slip system. *Phys. Rev. E* **63**, 061312 (2001)
- Dalton, F., Corcoran, D.: Basin of attraction of a bounded self-organized critical state. *Phys. Rev. E* **65**, 031310 (2002)
- Lynch, R., Corcoran, D., Dalton, F.: The onset to criticality in a sheared granular medium. In: *Recent Advances in Multidisciplinary Applied Physics*, vol 70, pp 369–373
- Liu, C.H., Nagel, S.R., Schecter, D.A., Coppersmith, S.N., Narayan, O., Witten, T.W.: Force fluctuations in bead packs. *Science* **269**, 513–515 (1995)
- Mueth, D.M., Jaeger, H.M., Nagel, S.R.: Force distribution in a granular medium. *Phys. Rev. E* **57**, 3164–3169 (1998)
- Mühlhaus, H.-B., Hornby, P.: On the reality of antisymmetric stresses in fast granular flows. In: *IUTAM Symposium on Mechanics of Granular and Porous Materials*, pp. 299–311. Kluwer Academic Publishers (1997)
- Ciamarra, M.P., Coniglio, A., Nicodemi, M.: Shear-induced segregation of a granular mixture under horizontal oscillation. *J. Phys. Condens. Matter* **17**(24), 2549–2556 (2005)